Progress In Electromagnetics Research, PIER 100, 299–308, 2010

A HIGH BAND ISOLATION AND WIDE STOPBAND DIPLEXER USING DUAL-MODE STEPPED-IMPEDANCE RESONATORS

C.-Y. Huang

Department of Electrical Engineering
National University of Tainan
33, Sec. 2, Shu-Lin St., Tainan 700, Taiwan

M.-H. Weng

Medical Devices and Opto-Electronics Equipment Department
Metal Industries Research & Development Center
3F, No. 88, Luke 5th Rd., Lujhu Township, Kaoshiung 82151, Taiwan

C.-S. Ye

Department of Electrical Engineering
Institute of Microelectronics
Advanced Optoelectronic Technology Center
National Cheng Kung University
No. 1, University Road, Tainan City 701, Taiwan

Y.-X. Xu

Department of Electrical Engineering
National University of Tainan
33, Sec. 2, Shu-Lin St., Tainan 700, Taiwan

Abstract—In this paper, a high performance diplexer is designed and fabricated for Global Positioning System (GPS) and wireless local area network (WLAN) applications simultaneously. The diplexer mainly comprises two dual-mode ring bandpass filters (BPFs), operated at 1.575 GHz and 2.4 GHz, respectively. By using the stepped-impedance resonator (SIR) in the BPFs, the size reduction and wide stopband from 2.8 GHz to 6 GHz are obtained. Moreover, several transmission zeros are located at the passband edges, thus improving the passband selectivity. Due to impedance matching between two BPFs, a high

Corresponding author: C.-Y. Huang (cyhun@mail.nutn.edu.tw).

isolation greater than 40 dB between two channels is obtained. The diplexer is investigated numerically and experimentally. The simulated and measured results have a good agreement with the proposed design concept.

1. INTRODUCTION

Diplexers are three terminal devices which let two or more frequencies into one input port and then separate them to two other output ports. For multi-service functions in modern wireless communication systems, compact-size and high performance diplexers are widely adopted [1–3]. In the past, several methods have been reported to develop diplexers [2–6]. For example, two periodic filter structures with open-circuited stubs are used to achieve a wide-band diplexer for multiple-frequency applications [2]. Two filters using common resonators sections [3] and with two matching circuits [5] are used to form a microstrip diplexer. In addition, two hairpin line filtering structures are used to form a UWB diplexer, and a tapped open stub is used to introduce an attenuation pole to suppress the spurious response and achieve a high isolation between two bands therefore [6]. However, in order to achieve the high isolation and a wide stopband simultaneously, the above mentioned diplexers in fact have some problematic issues, such as large dimension or high insertion loss.

In this paper, we propose a miniaturized band isolation and wide stopband microstrip diplexer used for Global Positioning System (GPS) of 1.575 GHz and Wireless Local Area Network (WLAN) of 2.4 GHz, respectively. Two square ring stepped impedance resonators (SIRs) [7–9] are used to realize miniaturized bandpass filters (BPFs) to satisfy the required passbands. Additionally, because of the appearance of the transmission zeros located at the passband edges, the high isolation between two passbands and a wide stopband are obtained simultaneously. Moreover, due to the good impedance matching in input port for two BPFs, a high isolation between two channels is also obtained. Measured results of the fabricated diplexer have a good agreement with the simulated results.

2. DESIGN PROCEDURE

Figure 1 shows the geometry structure of the proposed diplexer. The diplexer is designed on Duroid 5880 substrate having a thickness of 0.787 mm, a dielectric constant ε_r of 2.2, and a loss tangent of 0.0009. The BPFs in the proposed diplexer are two dual-mode

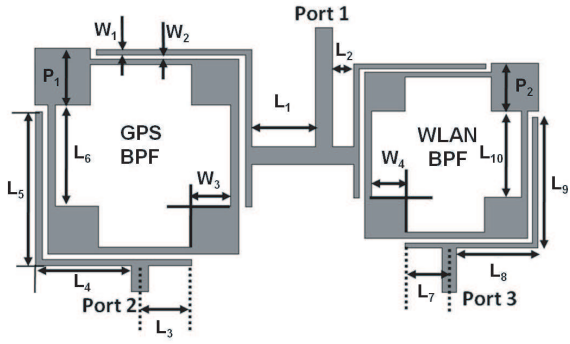

Figure 1. Schematic of the proposed diplexer.

BPFs, which are well known to have simple design procedure and good passband performance [10–12]. However, typical dual-mode BPF has disadvantages of large size and native harmonic responses. Therefore, by embedding the SIR in the dual-mode ring structure, the miniaturized size and spurious control can be solved simultaneously. The input line is coupled with two dual-mode SIR BPFs to provide the input power. To design the proposed diplexer, the following steps are used:

The first step is to discuss the equivalent circuit of the ring SIR as the basic filter block in the diplexer;

The second step is to analyze the resonant responses of the designed ring SIR;

The third step is to achieve the desired dual-mode band performances by using the designed ring SIR;

The fourth step is to combine the two BPFs with different center frequencies together to form two channels of the diplexer by tuning the coupling lines of the input port for impedance matching; and

The final step is to fabricate a sample and measure the performance.

In the first step, the equivalent circuit of the ring SIR as the basic filter block in the diplexer is discussed. Fig. 2 shows the layout and transmission-line model of the SIR in Fig. 1. The SIR is constructed by cascading a high-impedance section and low impedance section. The impedance ratio R is defined as $Z_{1//}/Z_2$. Since it is symmetry, as shown in Fig. 2(a), the resonant modes of the designed SIR can be modeled and calculated by the transmission-line theory. The input impedances (Z_{in1}) seen at the junction high-impedance section to the

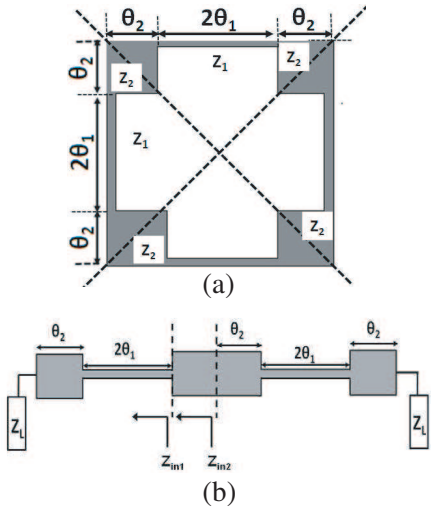

Figure 2. (a) Layout and (b) transmission-line model of the used ring SIR.

low-impedance section is derived as:

$$Z_{in1} = jZ_1 \frac{Z_2 \tan\theta_2 + Z_1 \tan 2\theta_1}{Z_1 - Z_2 \tan\theta_2 \tan 2\theta_1} \tag{1}$$

where θ_1 and θ_2 are electrical lengths of the high-impedance section and the fan-shaped low impedance section, respectively. Moreover, the input impedances (Z_{in2}) seen at the center of the SIR section is derived as:

$$Z_{in2} = Z_2 \frac{Z_{in1} + jZ_2 \tan\theta_2}{Z_2 + jZ_{in1} \tan\theta_2} \tag{2}$$

In the second step, we analyze the fundamental and higher order resonant frequencies of the designed SIR by using the (2). The odd and even resonances of the ring SIR occur when $Z_L = 0$ and ∞, respectively [13, 14]. The design parameters include impedance ratio (R) of the stepped sections and lengths. Proper choice of the above parameters leads to an optimal reduction of circuit dimension and extension of upper rejection bandwidth. Since the proposed diplexer design has two channels, thus the first BPF at 1.575 GHz require a wide upper stopband to avoid the interference of the second BPF at 2.4 GHz and the second BPF requires a wide lower stopband to avoid the interference of the first BPF.

Figure 3 shows the simulated results of the fundamental and first higher order resonant frequencies of the designed ring SIR of

the left side as shown in Fig. 1. The full-wave electromagnetic (EM) simulator [15] is used for simulation. When setting the $R = Z_{1/}/Z_2 = 4$, $\theta_1 = 22.5^\circ$ and $\theta_2 = 22.5^\circ$, the SIR can be designed for 1.575 GHz and the first spurious response is shifted far away to 6.5 GHz. By using the same totally physical length, the simulated results of the frequency response of the typical ring resonator 1 are also compared in Fig. 3. It is clearly observed that the fundamental resonant frequency of the typical ring resonator is at 2.1 GHz and many higher order resonant modes appear form 2 to 6 GHz. Similarly, Fig. 4 shows the simulated results of the fundamental and first higher order resonant frequencies of the designed ring SIR of the right side as shown in Fig. 1. When setting the $R = Z_{1/}/Z_2 = 4$, $\theta_1 = 22.5^\circ$ and $\theta_2 = 22.5^\circ$, the SIR can be designed for 2.4 GHz and the first spurious response is also shifted far away to 6.5 GHz. It is also clearly observed that the fundamental resonant frequency of the typical ring resonator 2 is at 3.1 GHz and many higher order resonant modes appear form 2.6 to 9.2 GHz. Based on the discussion, the designed SIR can be used to design dual-mode BPF with a miniaturized area and desirable wide stopband characteristics for the diplexer.

In the first step, the desired dual-mode band performances by using the designed ring SIR are addressed. To form the dual-mode

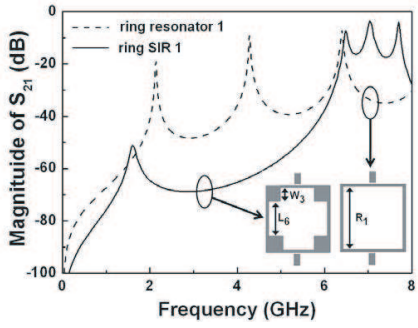

Figure 3. Simulated results of the fundamental and first higher order resonant frequencies of the designed ring SIR for GPS of 1.575 GHz and the typical ring resonator 1 with the same totally length. (The structural parameters as defined in Fig. 1 are: $L_6 = 14$, $W_3 = 6.4$, $R_1 = 2W_3 + L_6$, all in mm.).

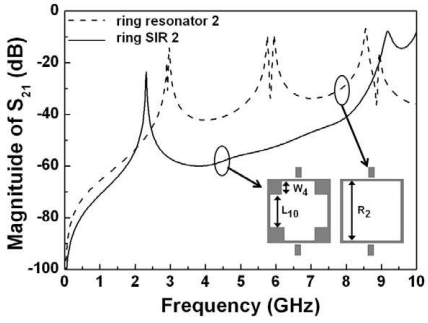

Figure 4. Simulated results of the fundamental and first higher order resonant frequencies of the designed ring SIR for WLAN of 2.4 GHz and the typical ring resonator 2 with the same totally length. (The structural parameters as defined in Fig. 1 are: $L_{10} = 9.2$, $W_4 = 5$, $R_2 = 2W_4 + L_{10}$, all in mm.).

BPF, the input and output ports shall be placed orthogonally near the proposed square ring SIR. Moreover, a perturbation element is located on the corner of the ring SIR. Since the proposed diplexer design has two channels, thus the first BPF at 1.575 GHz require a wide upper stopband to avoid the interference of the second BPF at 2.4 GHz and the second BPF requires a wide lower stopband to avoid the interference of the first BPF. Fig. 5 shows the simulated frequency responses of the designed dual-mode BPFs for GPS and WLAN without the matching network. By using the impedance ratio ($R = Z_{1/}/Z_2 = 4$) selected from Fig. 3 and carefully tunning the size of the perturbation element ($P_1 = 7.4$ mm), the first dual-mode BPF centred at 1.575 GHz has a fractional bandwidth of 3% and a harmonic suppression more than 20 dB up to 6 GHz, as expected in Fig. 3. In addition, the first dual-mode BPF has two transmission zeros located at 1.42 GHz and 1.67 GHz, with attenuation of 53 dB and 39 dB, respectively, thus much improving the band selectivity. Similarly, by using the impedance ratio ($R = Z_{1/}/Z_2 = 4$) selected from Fig. 4 and carefully tunning the size of the perturbation element ($P_2 = 6.1$ mm), the second dual-mode BPF centred at 2.4 GHz exhibits a fractional bandwidth of 8% and a harmonic suppression more than

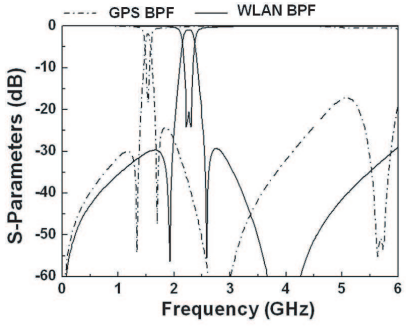

Figure 5. Simulated frequency responses of the designed dual-mode BPFs for GPS and WLAN without the matching network. (The structural parameters as defined in Fig. 1 are: $L_3 = 7$, $L_4 = 12.8$, $L_5 = 20.8$, $L_6 = 14$, $L_7 = 5.6$, $L_8 = 9$, $L_9 = 14.6$, $L_{10} = 9.2$, $W_1 = 0.2$, $W_2 = 0.2$, $W_3 = 6.4$, $W_4 = 5$, $P_1 = 7.4$, $P_2 = 6.1$, all in mm.).

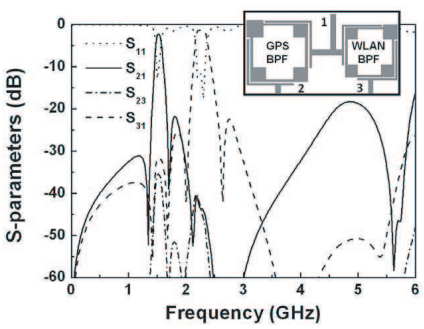

Figure 6. Simulated frequency responses of the proposed diplexer. (The structural parameters as defined in Fig. 1 are: $L_1 = 33.3$, $L_2 = 21.9$, $L_3 = 7$, $L_4 = 12.8$, $L_5 = 20.8$, $L_6 = 14$, $L_7 = 5.6$, $L_8 = 9$, $L_9 = 14.6$, $L_{10} = 9.2$, $W_1 = 0.2$, $W_2 = 0.2$, $W_3 = 6.4$, $W_4 = 5$, $P_1 = 7.4$, $P_2 = 6.1$, all in mm.).

30 dB up to 6 GHz, as expected in Fig. 4. Moreover, the second dual-mode BPF also has two transmission zeros located at 2.1 GHz and 2.69 GHz, with attenuation of 42 dB and 43 dB, respectively, which are expected to improve the isolation between two passbands.

Even the two designed passband performances satisfy the considered communication systems, it still has a challenge to combine the two BPFs together to form a diplexer without distortion of the passband performances. As shown in Fig. 1, the common input port is port 1, and the output ports for the first BPF and the second BPF are port 2 and port 3, respectively. In the fourth step, the two BPFs with different center frequencies are combined together to form the diplexer by tuning the coupling lines (L_1 and L_2) of the input port for impedance matching. The matching stub lengths L_1 and L_2 of the port 1 should be well designed to satisfy the following conditions. When the first BPF is operated, the input impedance seen into the second BPF is infinite. Likewise, when the second BPF is operated, the input impedance seen into the first BPF is infinite [4–6]. By the full-wave EM analysis, the stub lengths $L_1 = 33.3$ mm and $L_2 = 21.9$ mm are obtained for impedance matching, thus also achieving a high isolation $|S_{23}|$ greater than 50 dB between two channels. The simulated result of the diplexer by combining the two BPFs with matching network is shown in Fig. 6. It is clearly observed that several transmission zeros are still existed near the two passband edges in the designed diplexer, as obtained in two individual BPF shown in Fig. 5.

3. EXPERIMENTAL RESULTS AND DISCUSSION

In the final step, the proposed diplexer is then fabricated and measured by an HP8510C Network Analyzer. The photograph of the fabricated sample is shown in Fig. 7(a) and the measured results are displayed in Fig. 7(b). The first passband in diplexer has good measured results, including a center frequency of 1.575 GHz with $|S_{21}|$ of 2.5 dB, a lower stopband rejection greater than 18 dB beyond 1.6 GHz and a higher stopband rejection greater than 18 dB from 1.8 to 6.2 GHz. The second passband in diplexer also shows good measured results, including a center frequency of 2.45 GHz with $|S_{31}|$ of 1.4 dB, a lower stopband rejection greater than 18 dB beyond 2.2 GHz and a higher stopband rejection greater than 18 dB from 2.8 to 6.8 GHz. The loaded Q values are 18.3 and 13.1 for 1.575 GHz and 2.4 GHz, respectively. Due to the good impedance matching, the isolation between the two channels $|S_{23}|$ is better than 40 dB. In addition, the fabricated diplexer occupies a small size; around 30 mm $\times$ 70 mm. Measured results are slightly different from the simulated results. The mismatch could be

attributed to the unexpected inaccuracy during the fabrication [6]. The proposed diplexer actually has a good potential for the GPS and WLAN communication systems due to its simple design, compact size, and easy fabrication.

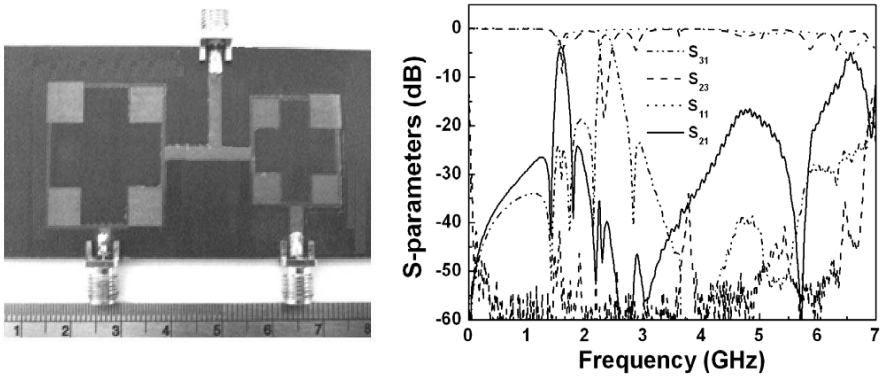

(a) (b)

Figure 7. (a) Photograph and (b) measured frequency response of the fabricated diplexer.

4. CONCLUSION

We have presented the design of a high performance diplexer for GPS of 1.575 GHz and WLAN of 2.4 GHz. Two dual-mode BPFs using ring SIRs are used as main blocks to form the proposed diplexer with a miniaturized size and a wide stopband. The design procedures are clearly discussed, including the equivalent circuit of the ring SIR, analysis of the resonant responses of the designed ring SIR, achieving the desired dual-mode band performances and tuning the coupling lines of the input port for impedance matching. Measured results show an insertion loss of 2.5 dB at 1.575 GHz with a lower stopband rejection greater than 18 dB beyond 1.6 GHz and a higher stopband rejection greater than 18 dB from 1.8 to 6.2 GHz; and an insertion loss of 1.4 dB at 2.45 GHz with a lower stopband rejection greater than 18 dB beyond 2.2 GHz and a higher stopband rejection greater than 18 dB from 2.8 to 6.8 GHz. Additionally, several transmission zeros are located near the passband edges to improve the isolation between two passbands. A high isolation greater than 40 dB between two channels is also obtained owing to the good impedance matching in the input port for two BPFs. Measured results of the fabricated diplexer have a good agreement with the simulated results.

REFERENCES

1. Yao, W. H., A. E. Abdelmonem, J. F. Liang, X. P. Liang, K. A. Zaki, and A. Martin, "Wide-band waveguide and ridge waveguide T-junctions for diplexer applications," *IEEE Trans. Microw. Theory Tech.*, Vol. 41, 2166–2173, 1993.
2. Strassner, B. and K. Chang, "Wide-band low-loss high-isolation microstrip periodic-stub diplexer for multiple-frequency applications," *IEEE Trans. Microw. Theory Tech.*, Vol. 49, 1818–1820, 2001.
3. Chen, C. F., T. Y. Huang, C. P. Chou, and R. B. Wu, "Microstrip diplexers design with common resonator sections for compact size, but high isolation," *IEEE Trans. Microw. Theory Tech.*, Vol. 54, 1945–1952, 2006.
4. Han, S., X.-L. Wang, Y. Fan, Z. Yang, and Z. He, "The generalized Chebyshev substrate integrated waveguide diplexer," *Progress In Electromagnetics Research*, Vol. 73, 29–38, 2007.
5. Deng, P. H., C. H. Wang, and C. H. Chen, "Compact microstrip diplexers based on a dual-passband filter," *Proceedings of Asia-Pacific Microwave Conference*, 2006.
6. Weng, M. H., C. Y. Hung, and Y. K. Su, "A hairpin line diplexer for direct sequence ultra-wideband wireless communications," *IEEE Microw. Wireless Compon. Lett.*, Vol. 17, 519–521, 2007.
7. Gao, S. S., X. S. Yang, J. P. Wang, S. Q. Xiao, and B. Z. Wang, "Compact ultra-wideband (UWB) bandpass filter using modified stepped impedance resonator," *Journal of Electromagnetic Waves and Applications*, Vol. 22, No. 4, 541–548, 2008.
8. Chin, K.-S. and D.-J. Chen, "Novel microstrip bandpass filters using direct-coupled triangular stepped-impedance resonators for spurious suppression," *Progress In Electromagnetics Research Letters*, Vol. 12, 11–20, 2009.
9. He, Z. R., X. Q. Lin, and Y. Fan, "Improved stepped-impedance resonator (SIR) bandpass filter in Ka-band," *Journal of Electromagnetic Waves and Applications*, Vol. 23, No. 8–9, 1181–1190, 2009.
10. Zhao, L.-P., X. Zhai, B. Wu, T. Su, W. Xue, and C.-H. Liang, "Novel design of dual-mode bandpass filter using rectangle structure," *Progress In Electromagnetics Research B*, Vol. 3, 131–141, 2008.
11. Dai, X.-W., C.-H. Liang, G. Li, and Z.-X. Chen, "Novel dual-mode dual-band bandpass filter using microstrip meander-loop resonators," *Journal of Electromagnetic Waves and Applications*,

Vol. 22, No. 4, 573–580, 2008.

12. Esfeh, B. K., A. Ismail, R. S. A. Raja Abdullah, H. Adamand, and A. R. H. Alhawari, "Compact narrowband bandpass filter using dual-mode octagonal meandered loop resonator for wimax application," *Progress In Electromagnetics Research B*, Vol. 16, 277–290, 2009.
13. Kuo, J. T. and C. Y. Tsai, "Periodic stepped-impedance ring resonator (PSIRR) bandpass filter with a miniaturized area and desirable upper stopband characteristics," *IEEE Trans. Microw. Theory Tech.*, Vol. 54, 1107–1112, 2006.
14. Choi, W. W. and K. W. Tam, "A microstrip SIR dual-mode bandpass filter with simultaneous size reduction and spurious responses suppression," *IEEE MTT-S International Microwave Workshop Series on Art of Miniaturizing RF and Microwave Passive Components*, Chengdu, China, 2008.
15. "IE3D Simulator," Zeland Software, Inc., 1997.
16. Thomson, N. and J. S. Hong, "Compact ultra-wideband microstrip/coplanar waveguide bandpass filter," *IEEE Microw. Wireless Compon. Lett.*, Vol. 17, 184–186, 2007.